OTKA K129142 _ 2018-2023

Final report

The research period of this OTKA grant has been extended for one Year due to consequences of the 2019 COVID pandemic (affecting seriously the 2020-21 experimental work) involving infections of participating colleagues, quarantine regulations, reduced animal facility services at both Budapest and Debrecen locations, and safety considerations to preserve resources with careful experimental scheduling. The delay was caused also by lost work forces, since the 2021-recruited young research fellow had to be excluded from the laboratory work after a short joint-period due to her high-risk pregnancy.

The extension period has been used to complete (1) the *in situ* hybridization experiments by determining the postnatal expression pattern of the NMDA receptor subunits NR2A and NR2B, the glycine receptor subunits GlyRa2 and GlyRa3, the glycine transporter 1 and the vesicular inhibitory amino acid transporter, (2) the electrophysiological recordings by running whole cell and gramicidin-perforated patch recordings combined with GABA and glycine uncaging, and optical stimulations of channel rhodopsin 2 expressing GLYT-2 fibers in the mouse basal forebrains, and (3) the behavioral tests (5 choice serial reaction time task – 5CSRTT) to detect potential changes generated by bilateral optical stimulation of glycinergic afferents of BF neurons.

These studies included double-, and triple transgenic mice expressing the Cre recombinase under the promoter activity of the glycine transporter-2 (GLYT2) gene and either enhanced green fluorescent protein (eGFP) in cholinergic neurons or channel rhodopsin-2/yellow fluorescent protein (ChR2/YFP) in glycinergic neurons or both eGFP and ChR2/YFP in triple transgenic mice.

I. Results of the neuroanatomical studies:

The ultrastructural examination of immunohistochemically double labeled BF sections revealed synaptic connections between glycinergic axon terminals and non-cholinergic neurons of the BF, such as parvalbumin, calbindin D-28K, calretinin neurons (**Fig.1.**), but not with somatostatin neurons (**Fig.2.**). To provide additional information and support for glycinergic signaling in non-cholinergic BF neurons, we have used immunofluorescent triple-labeling and confocal microscopy to determine the localization of non-cholinergic neurons together with the cholinergic neurons, and the presence of α subunits of glycine receptors in the phenotypically identified neurons. We have found glycine receptor immunoreactivity in close association with parvalbumin, calretinin and calbindin-immunoreactive neurons, but not with somatostatin neurons.

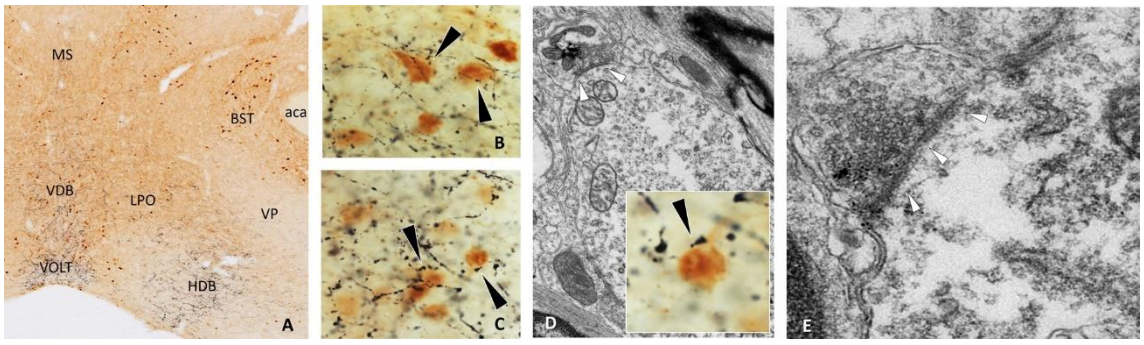

Fig. 1. *Immunohistochemical double-labeling for GLYT2 and CR in the mouse basal forebrain. (A) Calretinin neurons in the nucleus of the vertical limb of the diagonal band (VDB) are surrounded by a rich network of the GLYT2-IR axons. (B-C) At higher magnification, GLYT2-IR axons were found to appose (black arrowheads) calretinin-IR soma and dendrites. (D-E) Electron micrographs demonstrate synapses (white arrowheads) established by GLYT2-IR axon terminals on the postsynaptic cells immunolabeled for CR.*

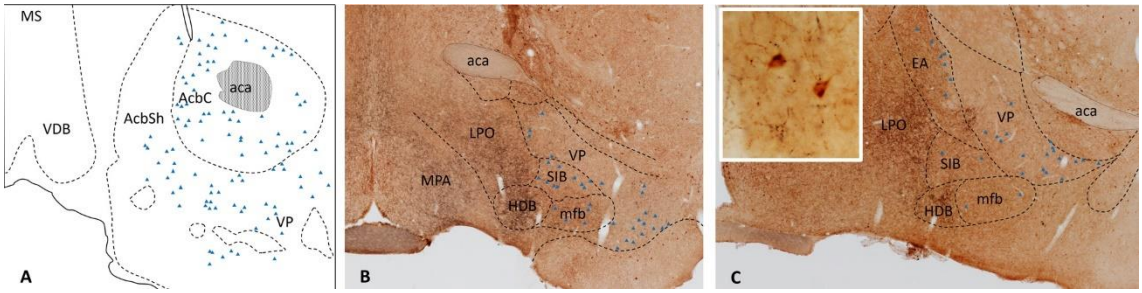

Fig. 2. *Immunohistochemical double-labeling for GLYT2 and SS in the mouse basal forebrain (Location of SS perikarya are marked by blue triangles). (A-C) Somatostatin neurons appear primarily in rostral BF regions. The GLYT2-IR fibers are rarely getting in connection with SS neurons; the inset shows the GLYT2-IR fibers (black arrows) in a distance from SS-IR perikarya.*

By using dual labeling immunohistochemistry, we showed that GLYT2-IR axons innervate calcium-binding protein-containing in the medial septum, VDB and horizontal limb of the diagonal band of Broca (HDB). Each of the investigated neuron-type was found to be associated with GLYT2-IR varicosities. In the medial septum fewer appositions were seen than in the VDB or the HDB. Somatostatin neurons are rarely associated with GLYT2-IR appositions (**Fig.2**).

By electron microscopic analyses we identified examples of GLYT2-IR axon terminals which made synapses onto calretinin (**Fig.1**), calbindin, parvalbumin-IR neurons in the VDB or HDB. The synapses found were symmetric between GLYT2-IR axons and calcium binding protein – containing neurons indicating their most likely inhibitory character.

II. Results of studies on the spatial and temporal expression of transcripts critically involved in glycine signalling:

Brains of wild-type or transgenic mice expressing eGFP in ChAT neurons were collected at four different postnatal (PN) time points (PN1, 7, 14, 45), flash frozen and cryosectioned to 14 µm-thick sections. Six consecutive sections 140 µm apart from each other were mounted onto a single glass slide to represent various cells and subdivisions of the basal forebrain. 5 slides from five different brains represented each of the experimental groups in the hybridization procedure (all together 20 slides). Slides were preselected for each hybridization experiment and stored in different boxes at -80 °C. The second version of the Multiplex RNAscope technique (with enhanced signal detection for 2-4 different mRNAs) was used to study the spatial-temporal expression of transcripts critical in glycine signaling. After hybridization, slides were coverslipped and scanned at 20x magnification in the Pannoramic slide scanner of 3DHistech Ltd. Regions of interest (subdivisions and perikarya of signal containing cells) were selected on digitalized images and exported for further analyses in Image J. Percentage of areas covered by thresholded pixels (representing the fluorescent signal), or number of grains within the ROIs were determined.

1. Expression of NKCC1 and KCC2 in the various subdivisions and cholinergic neurons of the basal forebrain.

First, we have focused on the expression of chloride transporters NKCC1 and KCC2, since a developmental shift in their increased/decreased expression in target cells of GABAergic/glycinergic afferents could critically influence the basal forebrain circuit activity. Their mRNA levels together with the transcripts of choline acetyl transferase (ChAT) were determined (**Fig.3D**). Transcripts of NKCC1, and KCC2 were detected in sections of all developmental stage investigated. The ChAT mRNAs level was, however, critically low at PN1, insufficient to study the NKCC1 and KCC2 co--expression in cholinergic neurons at this time point but were detected well in PN7 brains. Colocalization of ChAT signal with the NKCC1 and KCC2 was already observed at this time point, and the mRNA signals of KCC2 in ChAT cells increased significantly from PN7 to PN14 and PN14 to PN45 (**Fig.3B**). No postnatal downregulation could be observed, however, for NKCC1 expression in ChAT mRNA positive neurons, instead an increase of its level was detected reaching the highest level at PN45 ChAT neurons. This was in contrast with the regional decrease of NKCC1 transcript levels in the MS and HDB already detectable from PN7 (**Fig.3A**). The relatively strong transcriptional activity for KCC2 at PN14 suggests a potential change in the intracellular chloride concentration of cholinergic neurons around this developmental stage (**Fig.3C**). The gramicidin-perforated patch clamp experiments run parallel by the participant research group in Debrecen put this transition to PN12-13. The chloride reversal potential was found-45.07 ± 5,26 mV in juvenile animals (2-8 days old ones) and -71,4 ± 3,92 mV in adults (130-214 days old) (**Fig.11**)

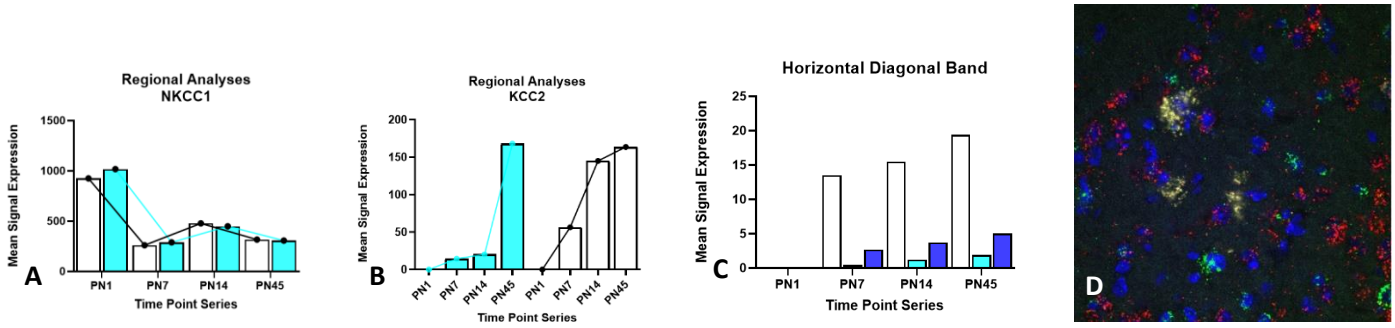

Fig. 3. *Regional and cellular expression of NKCC1 and KCC2 in the basal forebrain and ChAT neurons. A & B. Regional comparison of NKCC1 and KCC2 mRNA levels in the Medial Septum (MS) and Horizontal Diagonal Band (HDB). C. Expression levels of the chloride transporters in ChAT perikarya defined by ChAT mRNA signals. D. RNAscope fluorescent signals for NKCC1 (red), KCC2 (green), ChAT (yellow) mRNAs revealed single, double and triple labelled cells in DAPI counterstained sections. Colocalization of ChAT, KCC2, NKCC1 signals can be observed in the BFC neurons.*

2. Expression of glycine and NMDA receptor subunits in cholinergic neurons.

Glycine receptors are arranged as five subunits surrounding a central pore, with each subunit composed of four α helical transmembrane segments. There are presently four known isoforms of the ligand-binding α-subunit (α1-4) of GlyR (GLRA1, GLRA2, GLRA3, GLRA4) and a single β-subunit (GLRB). We have selected to study the expression of alpha two and three subunits, as receptors containing these subunits are abundant during development, have been found in extrasynaptic locations and considered to participate in diseases with attention deficits. In addition, there is a postnatal subunit change (from α2 to α1), but data support that α2 continues to be the dominating α-subunit in the forebrain of adult animals.

Results: In agreement with our previous immunohistochemical results, we localised GlyR α subunit mRNAs in ChAT-positive perikarya. The level of α3 subunit transcripts were relatively low during the first two weeks of postnatal life (PN1:3.94±0.95%, PN7:5.82±1.56%, PN14:4.42±1.26%) but it increased significantly in the cholinergic neurons of adult mice (12.68±1.8%).

The NMDA receptor forms a heterotetrametric between two GluN1 and two GluN2 subunits. Multiple receptor isoforms with distinct brain distributions and functional properties arise by selective splicing of the GluN1 transcripts and differential expression of the GluN2 subunits. GluN2 subunits are expressed differentially across various cell types and developmental timepoints and control the electrophysiological properties of the NMDA receptor. GluN2B is mainly present in immature neurons and in extrasynaptic locations. While GluN2B is predominant in the early postnatal brain, the number of GluN2A subunits increases during early development; eventually, GluN2A subunits become more numerous than GluN2B. This is called the GluN2B-GluN2A developmental switch. We studied the expression of these two subunits.

Results: The developmental switch does not seem to manifest in the cholinergic neurons, at least at transcript levels. Both NR2A and NR2B mRNAs are present in the cholinergic neurons with gradual and significant increase from PN1 to PN45 (5.77±0.52%, and 12.17±0.48%, respectively).

It is increasingly recognized that GABA is a fast neurotransmitter utilized throughout the forebrain cholinergic system. GABA/ACh corelease may have major implications in modulating cortical functions including attention. In concordance with this emerging concept, VGAT mRNA signal was detected in most ChAT mRNA containing perikarya, however, the level of the VGAT mRNAs were very low in early postnatal life (from PN1 to PN14, 0.81±0.56%, 1.23±0.47%, 1.52±1%, respectively). In contrast, all investigated cholinergic cells (100 cells) in the basal forebrain contained significantly increased level of VGAT transcripts in young adult animals (5.61±1.51%).

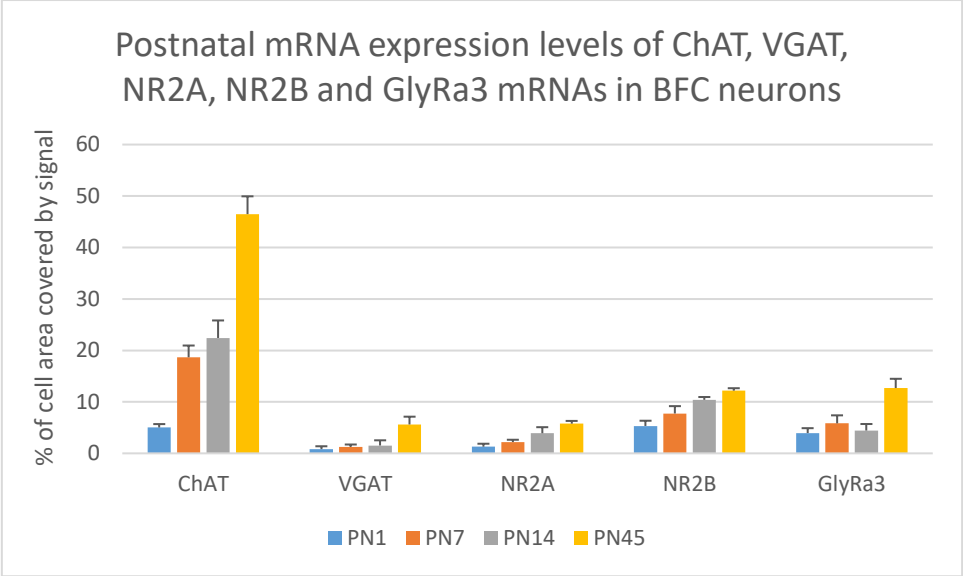

Fig.4. *Expression of VGAT, glycine and NMDA receptor subunit mRNAs in cholinergic neurons at four different times of postnatal life.*

3. Expression of glycine receptor subunits in non-cholinergic, GABAergic neurons

Expression of VGAT mRNAs in non-cholinergic neurons exhibited similar dynamics to those observed in BFC neurons. The mRNA levels were higher already from PN1 (2.93±0.51%), which stayed at a moderate level in PN 7 (4.81±0.88%) and 14 (4.5±1.12%) animals but exhibited more than a double value upon reaching young adulthood (11.83±2.5%).

Transcripts for both glycine receptor subunits were present in the VGAT mRNA positive neurons of the basal forebrain, indicating them being as target cells of glycine signaling. These data supplement our immunohistochemical data showing synaptic contacts of GLYT2-immunoreactive fibers onto various inhibitory cell types of BF.

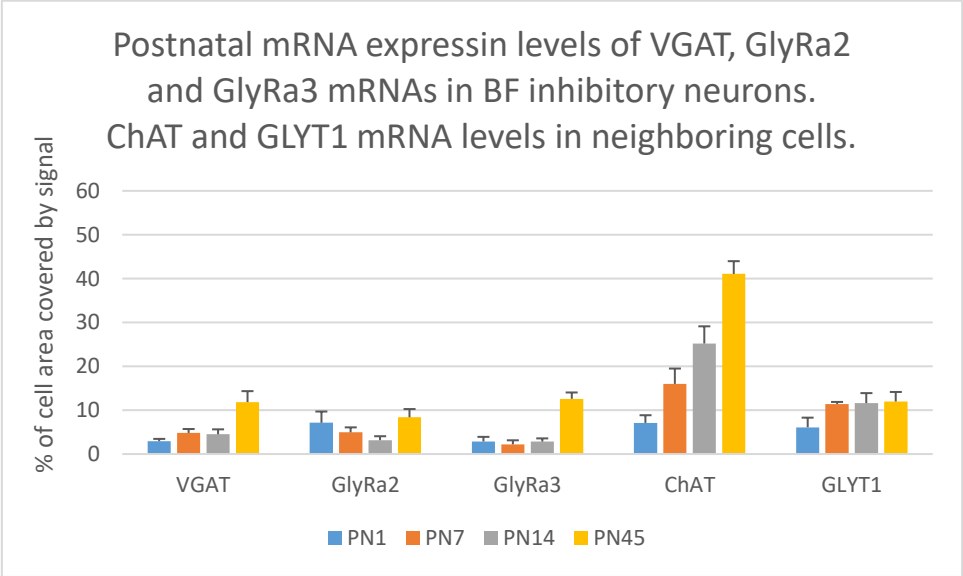

Fig. 5*. Expression of glycine receptor subunits in non-cholinergic, GABAergic neurons. Expression of Glycine transporter-1 in the vicinity of cholinergic neurons.*

4. Expression of Glycine transporter-1 in the vicinity of cholinergic neurons

The extracellular level of glycine in the brain is controlled by the type one glycine transporter (GlyT1), which is abundantly expressed already during the embryonic life. This transporter has been reported to be produced primarily by astroglia cells, the fine processes of which cover most of the non-synaptic surface of the neuronal processes in the neuropil. Sakers et al (PNAS, 2017) reported that astrocytic translation is carried out locally in their peripheral processes, which may explain GLYT1 mRNA expression detected in our hybridized section in close association with ChAT neurons. GLYT1 mRNAs (6.08±2.2%) are present in association with PN1 ChAT cells, the level of which reaches a

relatively high level in postnatal day 7 (11.39±0.48%), which is than maintained until young adulthood (11.97±2.17%). The intense GLYT1-immunoreactivity found in our earlier experiments in the vicinity of ChAT-IR neurons is supported by the strong transcriptional level detected here.

III. Results of the electrophysiological studies:

1. Effect of GLYT1 inhibition on the electrical properties of cholinergic neurons – prevalence of circadian influence

Concerning the very fast elimination of glycine from the extracellular space by the glial membrane transporters, and the presence of the fine astrocytic processes in the vicinity of glycinergic synapses as we have shown (***Bardóczi et al, JNeurosci, 2017***), direct bath application of glycine was not expected to evoke changes in target cells. Therefore, first we employed a specific inhibitor of GLYT1 i.e., LY2365109 hydrochloride, to elevate local extracellular glycine levels.

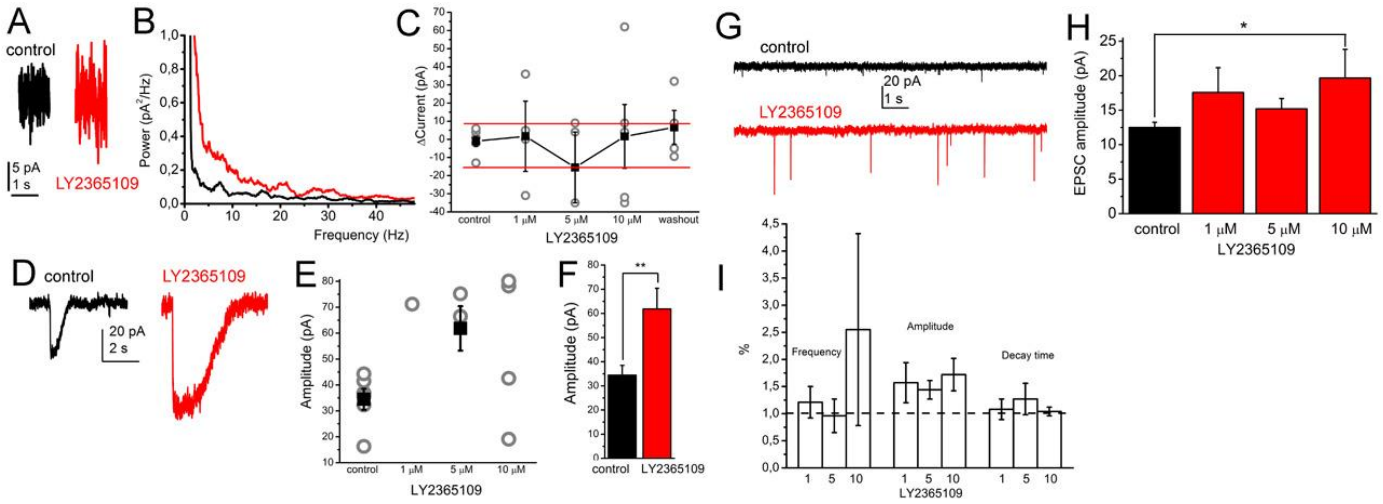

Fig.6. *Actions of GlyT1 inhibition on basal forebrain cholinergic neurons. A-B. Appearance of a reversible noise. A. Representative traces. B. Power spectra of traces before (black) and after application of glycine uptake inhibition (red). C. No clear tendency of appearance of tonic currents (gray circles: individual data, black squares: average ±SEM; red lines: fluctuations of the baseline). D-F. Astrocyte- and NMDA receptor-dependent slow inward currents (SICs) had a significantly increased amplitude. D. Representative SICs. E-F. Statistical summary of changes in SIC amplitude (gray circles: individual data, black squares and column diagrams: average ±SEM). G-I. There is a mild, statistically significant increase of sEPSC amplitude. G. Representative traces. H. Statistical summary of results with sEPSC amplitudes. I. Changes of sEPSC frequency, amplitude and decay tau normalized to control. (n= 5)*

This treatment resulted in an increase in the amplitude of the EPSCs. To clarify, whether direct glycinergic facilitation of signalling through NMDA receptors participate in this effect, an antagonist of the glycine binding site on the NMDA receptor (DCKA) has been administered to the perfusing solution.

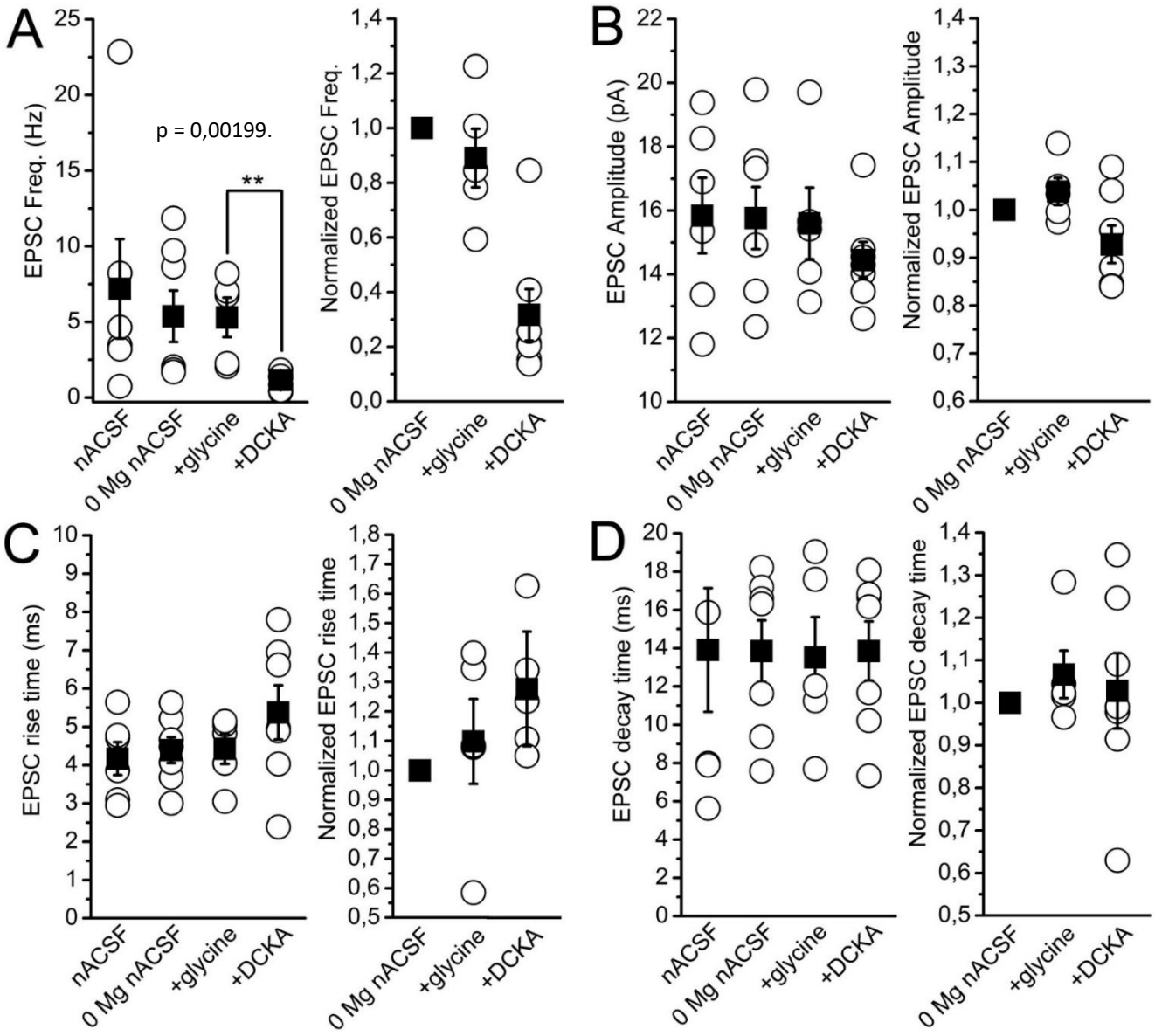

Fig.7. *Postsynaptic currents detected by whole-cell patch-clamp recordings in voltage clamp configuration characterized for amplitude and frequency under control conditions, and in the absence of Mg2+ and the presence of glycine, or an antagonist of the glycine binding site of the NMDA receptor (DCKA).*

Treatment with an antagonist of the glycine binding site on the NMDA receptor (DCKA) resulted in a significant reduction of the frequency of EPSCs, indicating a direct effect of glycine on the NMDA receptors of BFC neurons. Indirect effects, via disinhibiting cholinergic neurons, could also play a role in the elevation of EPSCs amplitudes. This possibility is supported by the current RNScope results showing expression of glycine receptor subunits (GlyRa2 and GlyRa3) by BF non-ChAT-positive, GABAergic neurons, and the synaptic contacts of GLYT2 immunoreactive fibers onto parvalbumin and calbindin immunoreactive cells.

As the BF is involved in the regulation of sleep-wake cycle, arousal state, and attentional processes of the experimental animals, we hypothesized a strong circadian influence on the activity and responsibility of the neuronal network involving the ascending glycinergic system of the brain stem. Therefore, we have studied the effects of the circadian cycle on synaptic and non-synaptic events of cholinergic BF neurons and on the actions of glycine transporter inhibition.

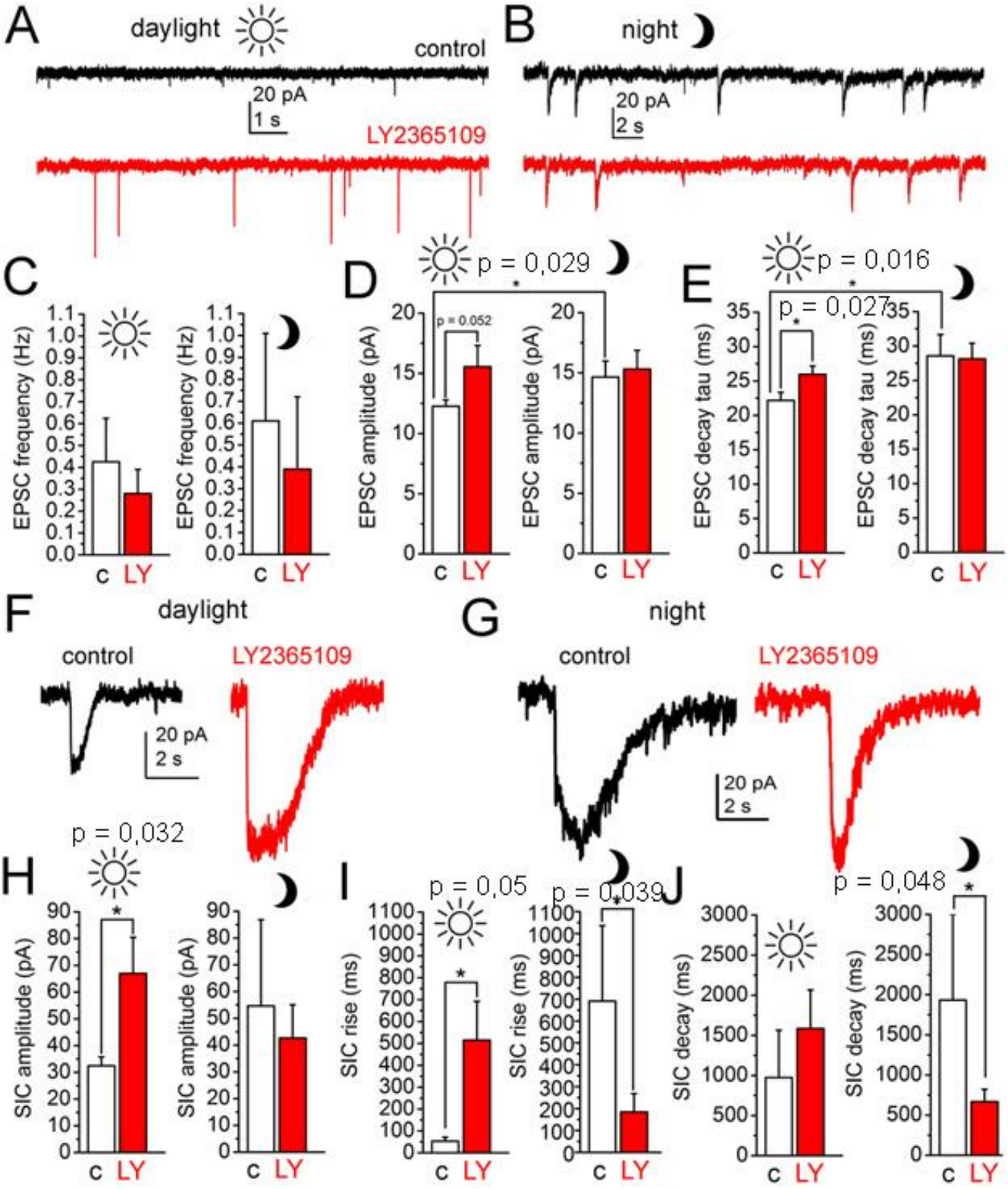

Fig.8. *Voltage clamp, whole cell recordings of cholinergic neurons of ChAT-tdTomato mice taken from samples collected either during the night or the day.*

These experiments revealed a significant circadian effect on the EPSCs of BFC neurons, showing significantly higher amplitude and longer decay time in slices of mice harvested during the night. Administering the GLYT1 inhibitor LY2365109, thus elevating the extracellular levels of glycine, resulted in an increased amplitude and decay time of EPSCs compared to controls only in slices collected during the day. The slow inward currents (SICs) known as excitatory events of neurons caused by astrocytic glutamate release and consequential activation of neuronal extra synaptic NMDA receptors, were differently influenced by the raised extracellular glycine levels. The amplitude and the rise time were increased in slices harvested during the day. In contrast, the rise time and the decay time were decreased in slices collected during the night.

2. Effect of local glycine release induced by optic stimulation on the electrical properties of cholinergic neurons.

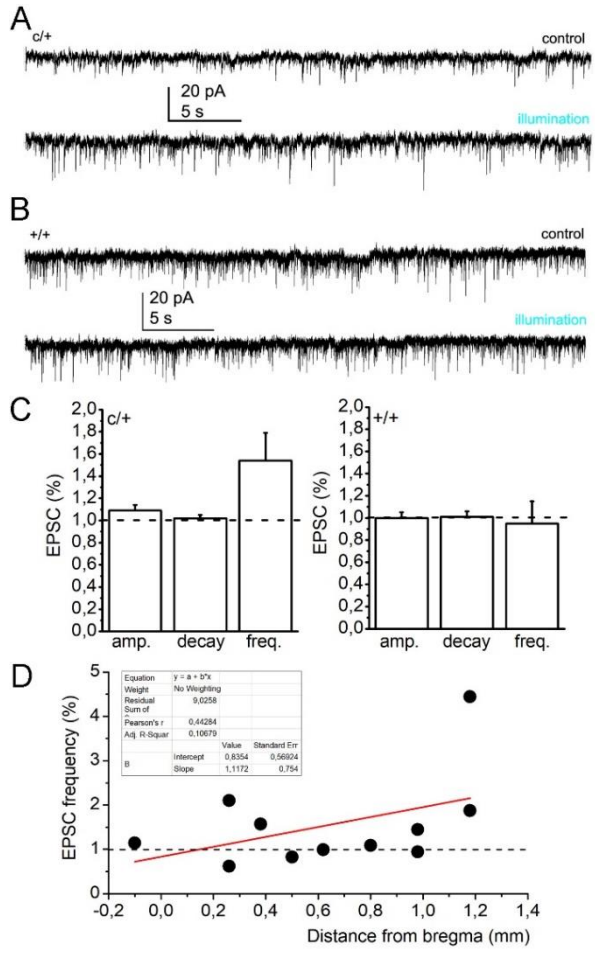

To study the effect of synaptically released glycine on the electrical properties of cholinergic and non-cholinergic neurons, slices of transgenic animals expressing channel rhodopsin-2 under the promoter activity of GLYT2 were used.

Fig.9. Optogenetic stimulation of the glycinergic fibers increase sEPSC frequency in the rostral regions of the BF. *A. Examples of current traces with sEPSCs before and during optogenetic stimulation ("illumination") in mice expressing the optogenetic actuator in glycinergic neurons (c/+). B. Examples of current traces with sEPSCs before and during optogenetic stimulation ("illumination") in mice with no expression of the optogenetic actuator (+/+). C. Percentages of changes in EPSC parameters in mice expressing the optogenetic actuator in glycinergic neurons (c/+) and with no expression of the optogenetic actuator (+/+).*

D. Correlation between the change of EPSC frequency by glycinergic stimulation and the distance of the neuron from the bregma (black dots: individual data, red line: linear fit).

The optogenetic stimulation (6,6 Hz) of the ChR2 expressing fibers resulted in a significant increase of the frequency of EPSCs.

IPSCs were also recorded (n=4). The frequency of the events increased from 0 to 1.06 Hz indicating a direct glycinergic effect on the cholinergic neurons. These *in vitro* experiments provided proof also of the functional presence of ChR2-expressing glycinergic fibers in the basal forebrain of the triple transgenic animals terminating on certain neurons.

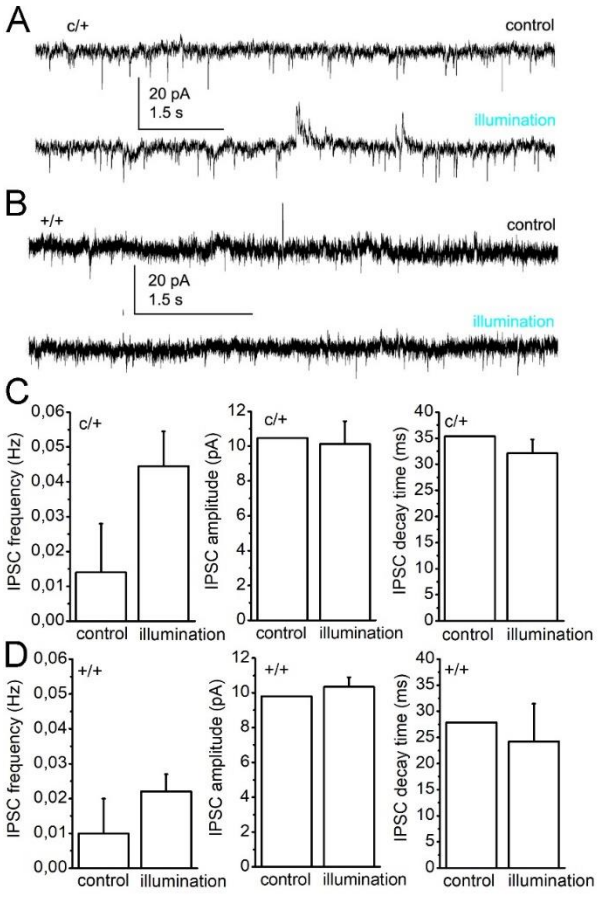

Fig.10. Optogenetic stimulation of the glycinergic fibers cause a tendency of sIPSC frequency increase*. A. Examples of current traces with sEPSCs and sIPSCs before and during optogenetic stimulation ("illumination") in mice expressing the optogenetic actuator in glycinergic neurons (c/+). B. Examples of current traces with sEPSCs (and a few small sIPSCs) before and during optogenetic stimulation ("illumination") in mice with no expression of the optogenetic actuator (+/+). C. Statistical comparison of sIPSC parameters in mice expressing the optogenetic actuator in glycinergic neurons (c/+). D. Statistical comparison of sIPSC parameters in mice with no expression of the optogenetic actuator (+/+).*

3. **Studies on the reversal potential of GABA and alteration of chloride concentration during the postnatal period.**

Prior to gramicidin-perforated patch experiments, we recorded cholinergic neurons in whole cell configuration by uncaging GABA at various holding potentials from -100 to +20 mV. When glycine was uncaged (n = 3), no current was recorded on the cholinergic neurons (with no clear explanation for the failure, yet).

Considering the chloride concentrations of the normal aCSF and the pipette solution, we calculated -82,18 mV as the expected reversal potential of chloride. The reversal potential of the GABA current based on our whole cell patch clamp recordings was -75,35 ± 5,18 mV.

In further experiments, gramicidin perforated patch recordings were done on 14 BF neurons, both on cholinergic and non-cholinergic ones. The reversal potential of the GABA currents was determined by using voltage steps from -100 to +20 mV with 20 mV increment, while flash photolysis was achieved in the middle of the voltage steps. Based on the Nernst equation (and on the hypothesis that no GABAB receptor activation occurred), the intracellular chloride concentration was also calculated. We found that the chloride reversal potential was -45.07 ± 5,26 mV in juvenile animals (2-8 days old ones) and -71,4 ± 3,92 mV in adults (130-214 days old), which significantly differed from each other (p = 0.0008). Calculated intracellular chloride concentrations were 25.07 ± 5.38 and 8.43 ± 1.17 mM in the different age groups (p = 0.005). Linear fitting of the datasets revealed a linear correlation of the age and the chloride reversal potential (r2 = -0.74 for the reversal potential and -0.65 for the calculated chloride concentration).

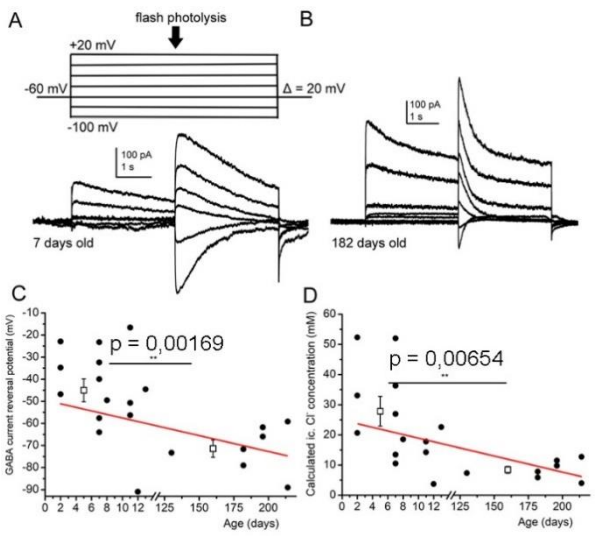

Fig.11. An age-dependent decrease of the initially higher intracellular chloride concentration was revealed on basal forebrain cholinergic and non-cholinergic neurons. *A. The protocol for GABA uncaging. While employing a protocol with voltage steps from -100 to +20 mV, flash photolysis of caged GABA was achieved by using a flash lamp (Rapp OptoElectronic, Wedel, Germany). A representative current trace of a neuron from juvenile mouse is seen below the protocol. B. A representative current trace from a neuron of an adult mouse. C. Statistical representation of the calculated GABA reversal potential. Black dots: individual data, hollow squares: averages of mice between 2-8 and 130-214 days. Red line: linear fit of the dataset. D. Intracellular chloride concentrations calculated by using the Nernst equation and by assuming no contamination by $GABA_B$ receptor activation. Black dots: individual data, hollow squares: averages of mice between 2-8 and 130-214 days. Red line: linear fit of the dataset. **: p*

Cholinerg and non-cholinerg neurons did not show any difference in this respect (GABA reversal potentials were -67,5 +-3 mV and -69,9 +-9,55 mV, respectively, p = 0,37).

IV. Results of the behavioral studies:

To study the potential effect of glycine in the basal forebrain released in response to optical stimulation of the channelrhodopsin-2 (ChR2) bearing glycinergic fibers, we have implanted micro-LEDs for ChR2 positive and ChR2 negative (control) animals next to their horizontal limb of the diagonal band of Broca (HDB)/substantia innominate/ventral pallidum (Si/VP) (n=8-8) or the medial forebrain bundle containing the ascending glycinergic fibers (n=4-4). After one week recovery time, the animals were trained in our automated training system in pairs (ChR2 positive and ChR2 negative animals) to get familiar with the 5CSRTT as described by *Birtalan et al. (Scientific Reports, 2020).* After a week training the animals reached a level of experience, at which they could react fast to the signal marking the location of their water-reward. This test was expected to give feedback about the animals' attention, alertness and learning processes.

First, we tested the potential effect of glycine on the attention of animals after one-week training. Precisely, whether optical stimulation at various frequency can alter the parameters characterizing each animal performance to drink water at the marked location. The following parameters were analyzed: **accuracy** (percentage of correct choice vs correct plus incorrect choices), **omission rate** (percentage of missed trials vs all trials) and the **reaction time**.

The first two pairs of animals (male and female pairs) received in our preliminary studies a unilateral micro-LED in the vicinity of HDB. The third pairs (male animals) received bilateral implants, which were first marketed in 2022. Concerning the inhibitory character of the ascending glycinergic pathways, using bilateral stimulus was a reasonable development in the experimental design. Introduction of micro-LEDs capable of providing bilateral stimulus, required the development of new tools, which ensures firm holding and perpendicular position of the shafts of the micro-LEDs in the stereotaxic instrument and the precise targeting of brain areas. Not having initially such holders, we have developed our own one which can hold concurrently both shafts, lower them together in the brain tissue, and hold them while the shafts are fixed to the skull. Later, Neurolux also marketed their renewed holder, by which the micro-LED bearing pins can be lowered one after the other one. The availability of a special gel glue, which can be applied precisely through a syringe needle to the cranial hole accepting the pins and start to cure only upon application of its own accelerator has greatly facilitated the type of implantation we needed targeting brain areas as deep as 5.5 mm from the bone surface. The target position left only a small gap between the holder and the skull to fix the 6 mm-long pin into the drilled hole.

(1) Learning of the task in the automated system is very fast. The animals increase their trial number and accuracy very fast but reaching a maximum usually by the third-fourth days, the accuracy drops, and omission of the trials increase a little bit with time. Variations in learning the task, and sudden changes in the performance of individual animals can be observed.

(2) Unilateral optical stimulus was ineffective to change the accuracy and omission levels of the ChR2 positive animal. Analyses of the behavioral test, which include histological processing of the brain (**Fig.13**) after removing the implants i.e. counterstaining of 40 µm-thick coronal sections, immunohistochemistry for GLYT2 and ChAT, are currently on completion for the animals received bilateral implants. The example below shows the accuracy level reached before the first light stimulus (mean of the last 12 trial sessions), while the target brain area is illuminated (30 Hz) (mean of the first 12 sessions), during the post-stimulatory period (mean of the first 12 sessions after the light stimulation), and finally, when the light stimulation was turned on again to provide timely signal for generating c-FOS expression in responsive cells (mean of the first 12 sessions). Comparison of values obtained from the expected light-responsive animal (Exp-3689), and the non-responsive animal (Ctrl-3688). The Exp-3689 animal shows an increased accuracy level and increased omission rate during the light stimulus, in contrast, the control animal exhibits a reduced accuracy level, and a reduced omission rate during the first light stimulus (**Fig.12**). Further analyses of the data are under way, including examination of potential day-night variations in the performance.

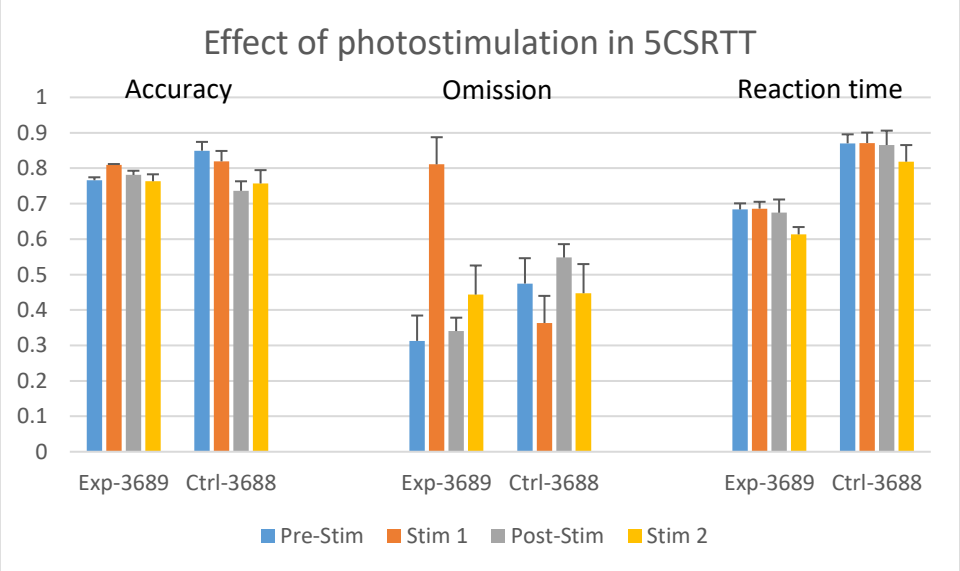

Fig.12. *Accuracy, omission rate and reaction time of channel rhodopsin 2-expressing (Exp-3689) and non-expressing (Ctrl-3688) animals before, during and after photo stimulation of the HDB region.*

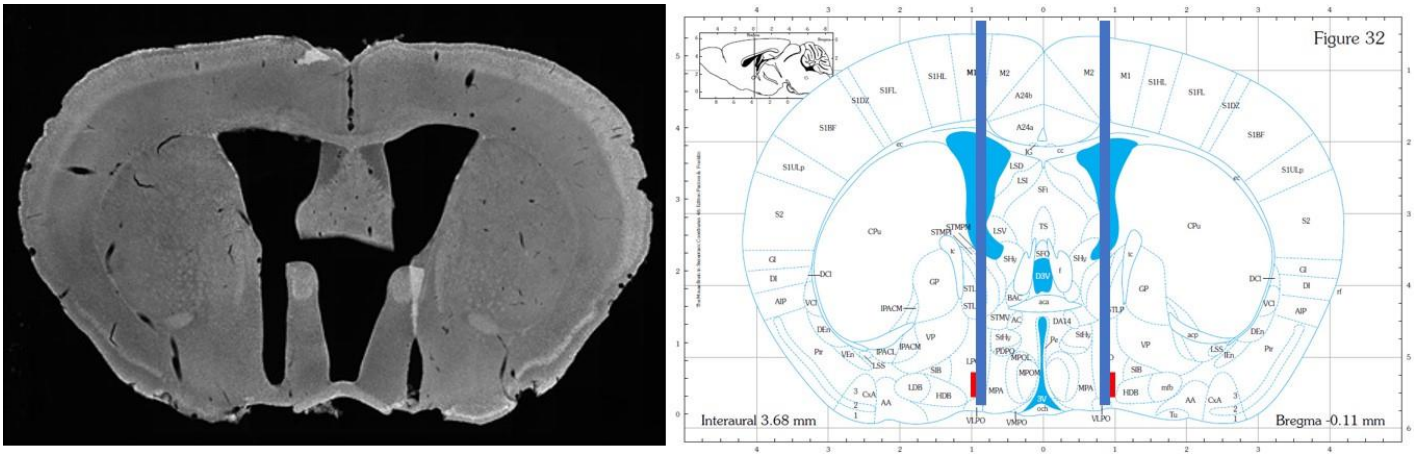

Fig.13. A brain section of animal Exp-3689 showing the tracks generated by the Micro-LED bearing pin in a position. This allowed the stimulus of ChR2 expressing fibers innervating the HDB.

Summary of our results:

1. Basal forebrain non-cholinergic neurons (i.e., parvalbumin, calretinin and calbindin neurons) were identified synaptically connected to ascending glycinergic fibers.

2. Postnatal expression of transcripts critically involved in glycine signaling (glycine and NMDA receptors, and GLYT1) were characterized in different subdivisions and cholinergic / non-cholinergic inhibitory cells of the basal forebrain.

3. The chloride reversal potentials, and its postnatal transition period in ChAT neurons has been determined. These were based on the cell-type specific analyses of the expression of chloride transporters, and the GABA uncaging, gramicidin perforated patch clamp recordings.

4. Circadian-dependent responses of the cholinergic neurons were demonstrated at circumstances of elevated extracellular glycine levels (by inhibition of GLYT1).

5. Distinct behavioral response was observed in 5CSRTTattention tests between animals capable or not capable of releasing glycine upon photo stimulation in the basal forebrain.

These results are waiting for publication, because we are trying to meet the expectation of the current publication policy of our Institute, which prefers aiming Nature-indexed journals with new observations and recommend completing studies to reach their scientific levels.

References:

Bardóczi Z, Pál B, Kőszeghy Á, Wilheim T, Watanabe M, Záborszky L, Liposits Z, Kalló I. (2017) Glycinergic Input to the Mouse Basal Forebrain Cholinergic Neurons. J Neurosci. 2017 Sep 27;37(39):9534-9549. doi: 10.1523/JNEUROSCI.3348-16.2017. Epub 2017 Sep 5. PMID: 28874448

Birtalan E, Bánhidi A, Sanders JI, Balázsfi D, Hangya B. (2020) Efficient training of mice on the 5-choice serial reaction time task in an automated rodent training system. Sci Rep. 2020 Dec 21;10(1):22362. doi: 10.1038/s41598-020-79290-2. PMID: 33349672

Sakers K, Lake AM, Khazanchi R, Ouwenga R, Vasek MJ, Dani A, Dougherty JD. (2017) Astrocytes locally translate transcripts in their peripheral processes. Proc Natl Acad Sci U S A. 2017 May 9;114(19):E3830-E3838. doi: 10.1073/pnas.1617782114. Epub 2017 Apr 24. PMID: 28439016